Supplement of Atmos. Chem. Phys., 21, 5965–5982, 2021
https://doi.org/10.5194/acp-21-5965-2021-supplement

Atmospheric Chemistry and Physics
Open Access
EGU

Supplement of

Aerosol radiative forcings induced by substantial changes in anthropogenic emissions in China from 2008 to 2016

Mingxu Liu and Hitoshi Matsui

Correspondence to: Hitoshi Matsui (matsui@nagoya-u.jp)

Table S1. Information of observation sites for sulfate, nitrate, and black carbon concentrations used for model evaluation. EANET, Acid Deposition Monitoring Network in East Asia.

Site	Species	Year	Lon (°)	Lat (°)	References
Beijing	Sulfate, Nitrate	2006/2008/2010	116.33-116.37	39.95-39.99	Zhang et al. (2013), Hu et al. (2016), Sun et al. (2010), Huang et al. (2010)
Beijing	Sulfate, Nitrate	2016	116.32	39.95	Liu et al. (2018)
Beijing	BC	2008-2016	116.37	39.97	Xia et al. (2020)
Zhengzhou	Sulfate, Nitrate	2010	113.52	34.8	Geng et al. (2013)
Tianjin	Sulfate Nitrate	2008	117.17	39.01	Gu et al. (2013)
Nanjing	Sulfate	2015	118.71-118.75	32.01-32.21	Ge et al. (2017), Wang et al. (2016), Zhang et al. (2017)
Hangzhou	Sulfate	2016	120.21	30.21	Li et al. (2018)
Chengdu	Sulfate, Nitrate	2006	104.04	30.65	Zhang et al. (2012)
Changde	Sulfate, Nitrate	2006	111.71	29.17	Zhang et al. (2012)
Jinsha	Sulfate, Nitrate	2006	114.2	29.63	Zhang et al. (2012)
Shanghai	BC	2008-2016	121.59	31.18	Wei et al. (2020)
Fukue Island	BC	2010-2016	128.68	32.75	Kanaya et al. (2019)
Xiamen	Sulfate, Nitrate	2008, 2016	118.13	24.47	EANET
Rishiri	Sulfate, Nitrate	2008, 2016	141.20	45.12	EANET
Ochiishi	Sulfate, Nitrate	2008, 2016	145.50	43.15	EANET
Tappi	Sulfate, Nitrate	2008, 2016	140.35	41.25	EANET
Sado-seki	Sulfate, Nitrate	2008, 2016	138.40	38.23	EANET
Happo	Sulfate, Nitrate	2008, 2016	137.80	36.70	EANET
Ijira	Sulfate, Nitrate	2008, 2016	136.68	35.57	EANET
Oki	Sulfate, Nitrate	2008, 2016	133.18	36.28	EANET
Hedo	Sulfate, Nitrate	2008, 2016	128.25	26.87	EANET
Tokyo	Sulfate, Nitrate	2008, 2016	139.75	35.68	EANET

Table S2. Comparison of modeled surface sulfate and nitrate concentrations in $PM_{2.5}$ (in parentheses) with corresponding observations at available sites shown in Table S1 during 2008 and 2016. Note that even in the same city, the observation site and associated sampling methods were likely different during the study period.

	Sulfate ($\mu g\ m^{-3}$)		Nitrate ($\mu g\ m^{-3}$)	
City	2008	2016	2008	2016
Beijing	15.8 (17.8)	8.70 (6.86)	13.2 (6.42)	10.8 (12.9)
Nanjing	-	5.70 (8.15)	-	-
Tianjin	19.1 (31.4)	-	12.0 (9.39)	-
Zhengzhou	25.7 (33.8)	-	16.7 (10.8)	-
Chengdu	40.5 (21.5)	-	15.1 (6.68)	-
Changde	28.8 (20.9)	-	8.5 (10.1)	-
Jinsha	26.6 (15.2)	-	7.2 (4.80)	-
Hangzhou	-	5.60 (5.95)	-	-
Xiamen	13.4 (5.40)	10.7 (3.69)	7.80 (2.36)	7.16 (3.34)
Rishiri	2.94 (2.12)	2.04 (1.64)	0.76 (0.33)	0.63 (0.49)
Ochiishi	2.73 (1.73)	1.94 (1.33)	0.71 (0.48)	0.66 (0.66)
Tappi	4.64 (3.43)	3.07 (2.65)	1.25 (0.81)	1.30 (1.11)
Sado-seki	4.17 (4.59)	2.84 (3.55)	1.09 (0.48)	1.02 (0.71)
Happo	2.53 (4.70)	1.75 (3.89)	0.25 (1.18)	0.37 (1.52)
Ijira	4.82 (4.74)	2.88 (4.01)	0.40 (1.53)	0.46 (1.86)
Oki	4.54 (7.09)	4.65 (5.52)	1.20 (0.48)	1.93 (1.06)
Hedo	6.03 (6.16)	4.54 (5.15)	1.60 (0.02)	1.60 (0.12)
Tokyo	5.21 (6.08)	3.22 (5.41)	4.05 (0.61)	3.22 (0.81)

Table S3. China's historical emissions for 2016 and the future emission scenario SSP1-RCP2.6-BHE for 2030 and 2050 provided by Tong et al. (2020)

Unit: Tg	2016	2030	2050	2030/2016	2050/2016
BC	1.3	0.49	0.28	0.38	0.22
SO_2	13	5.9	2.3	0.44	0.17
NO_x	23	10	6.1	0.46	0.27
OC	2.3	1.2	0.66	0.50	0.29
VOC	28	20	13	0.70	0.45
$PM_{2.5}$	8.1	3.9	2.0	0.48	0.24
NH_3	10	8.5	6.1	0.85	0.61
CO	142	92	69	0.65	0.49

Table S4. Differences of changes in BC and sulfate burdens and their DRF estimates between the Exp08-Exp16 and Exp08-Exp16m cases over eastern China. The Exp08-Exp16 represents the influences of only the variation in anthropogenic emissions during 2008–2016 and the Exp08-Exp16m represents the joint influences of emissions and meteorological conditions.

	Differences of burdens (mg m^{-2})		Differences of DRF (W m^{-2})	
	Exp08-Exp16	Exp08-Exp16m	Exp08-Exp16	Exp08-Exp16m
BC	−0.36	−0.33	–0.33	−0.24
SO_4^{2-}	−7.0	−6.5	0.58	0.55

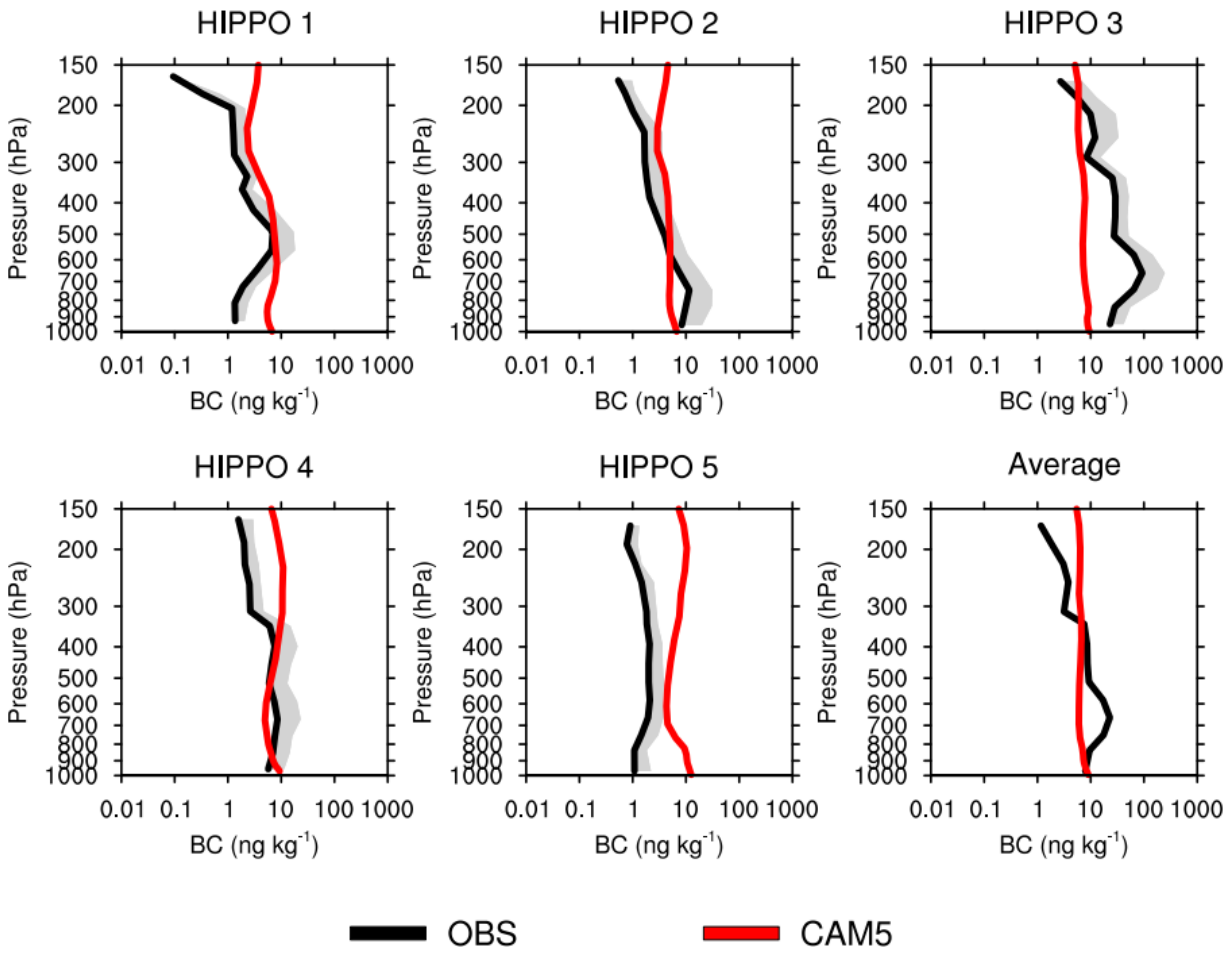

Fig. S1 Comparison of simulated vertical BC concentration profiles in the year 2008 with observations from five HIPPO campaigns during 2009–2011 over northern Pacific Ocean. The monthly mean BC concentrations in our simulation were obtained at the same months with the HIPPO observations but in different years. Both observations and simulations were averaged in the region of 160 ℃E–150 ℃W and 20 ℃N-60 ℃N. The grey colors denote the positive standard deviations of observations.

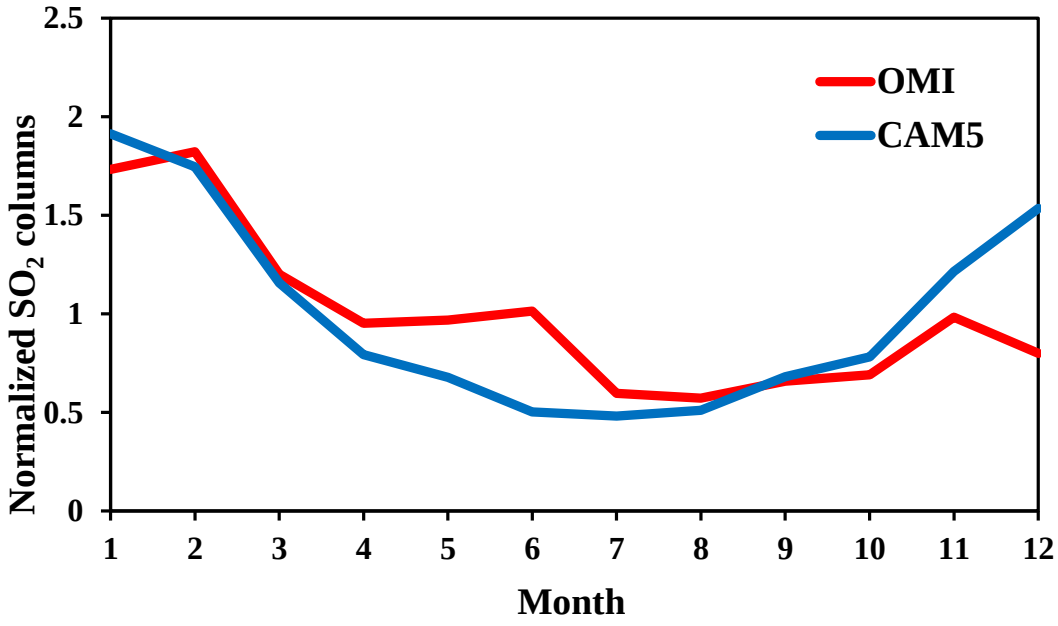

Fig. S2 Comparison of monthly cycles of normalized SO_2 columns in East China between OMI and CAM5 for the year 2008. The normalized SO_2 values were obtained from the corresponding monthly SO_2 column concentrations dividing by their annual mean for both simulations and observations. Because OMI measurements were provided once a day around 1:45 p.m. local time and CAM5 results were monthly averaged, we used the normalized results for the comparison to reduce the bias introduced by the inconsistency of sampling intervals.

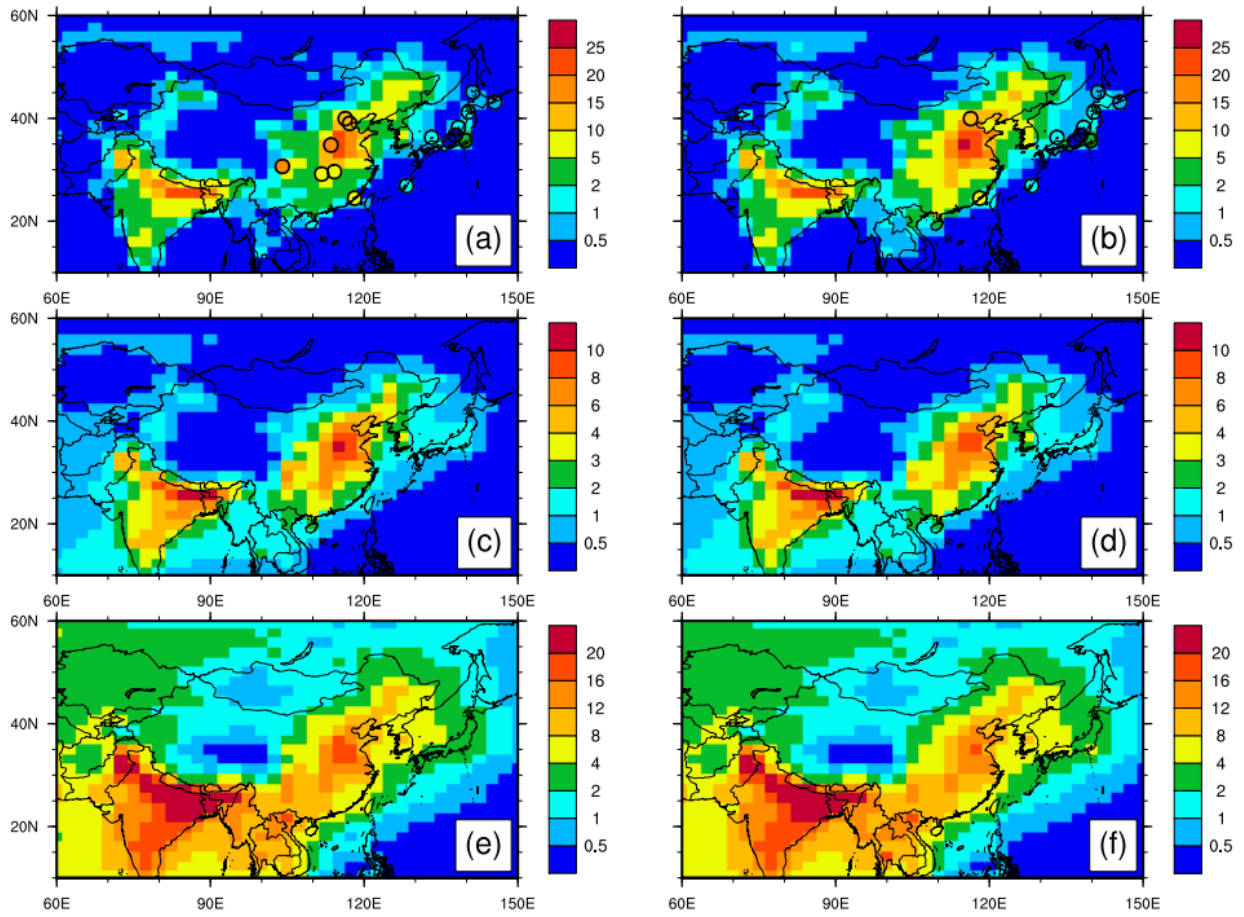

Fig. S3 Simulated annual mean surface concentrations (unit: μg m^{-3}) of $PM_{2.5}$ nitrate (a-b), ammonium (c-d), and organic aerosols (e-f) between emission years 2008 (left) and 2016 (right). Measurements of nitrate concentrations are shown in colored dots for comparison.

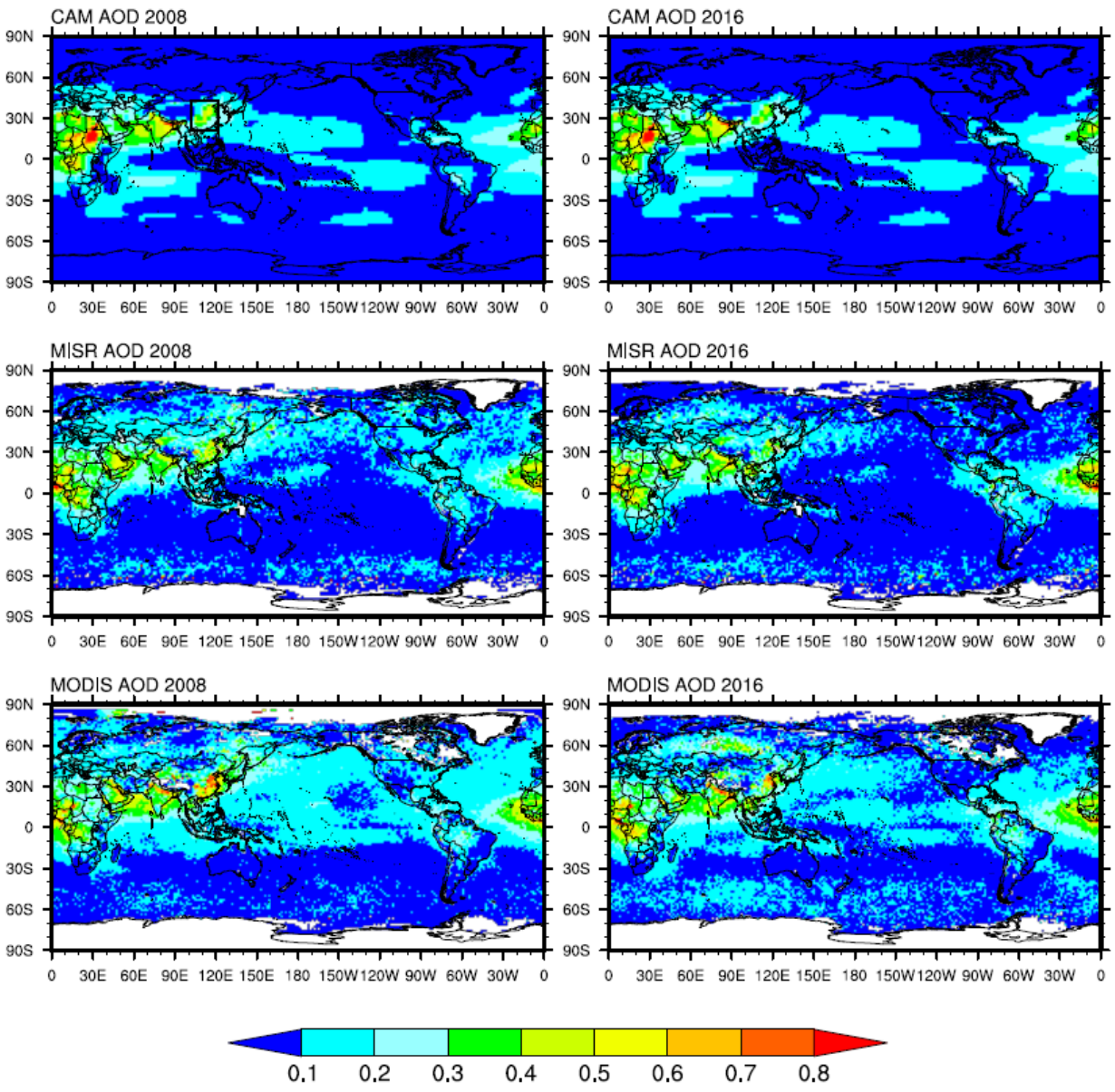

Fig. S4 Comparison of modeled AOD at 550 nm with MISR and MODIS observations in the years 2008 and 2016. Note that the modeled annual mean AOD for 2016 was derived from the simulation using the anthropogenic emissions in 2016 for China and the emissions in 2008 for other countries. The areas without the observation records are show in white color.

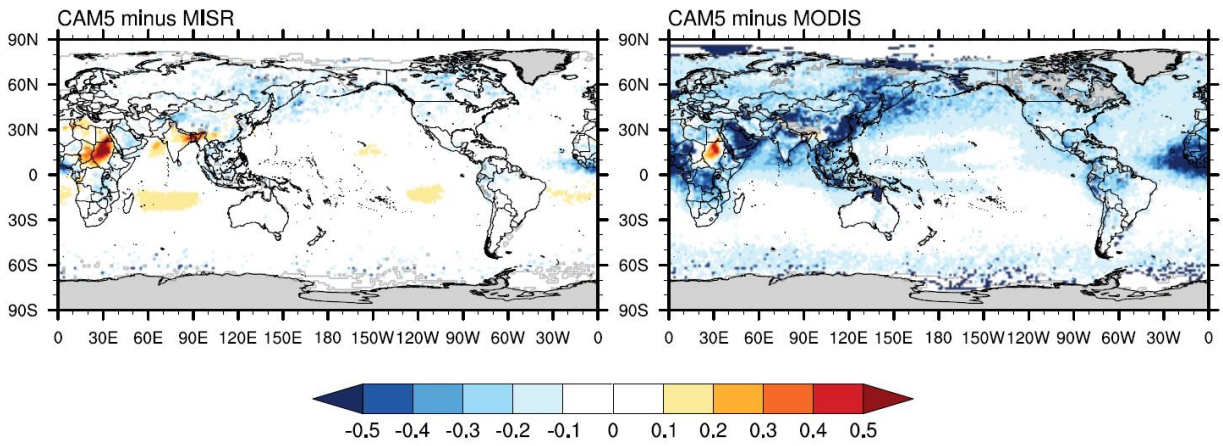

Fig. S5 Absolute differences between modeled annual mean AOD at 550 nm and the corresponding observations from MISR (left) and MODIS (right) for 2008.

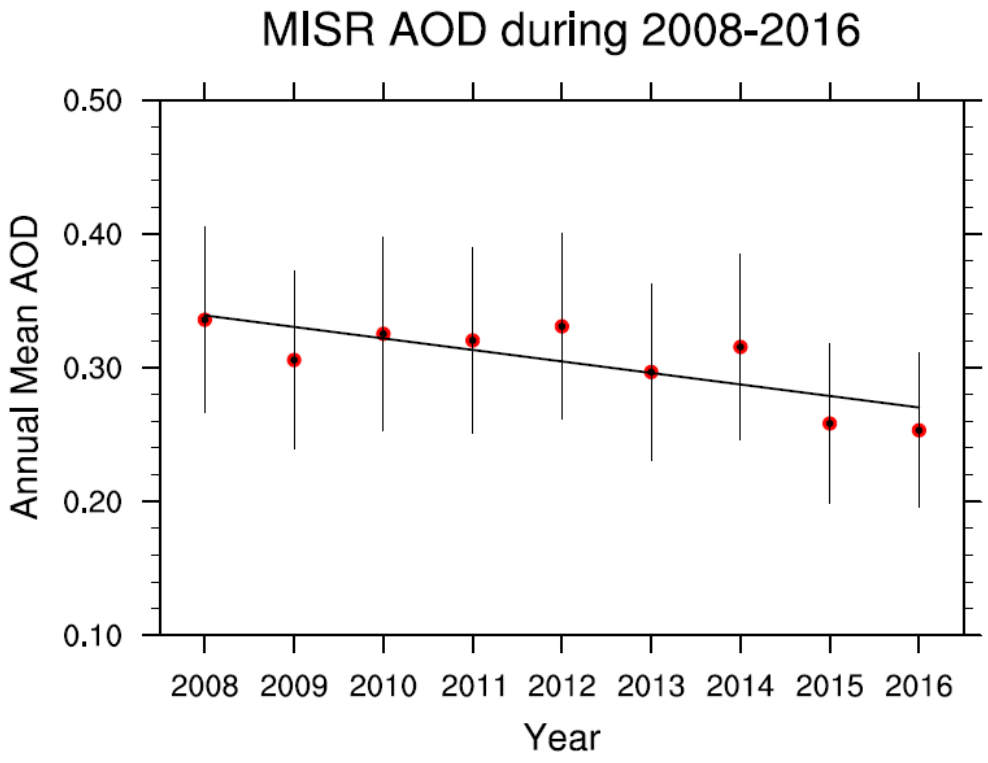

Fig. S6 Inter-annual variation in AOD at 550 nm retrieved by MISR over eastern China during 2008–2016. The mean values (dots) and standard deviations (vertical lines) were calculated using the gridded AOD and standard deviation from the Level-3 MISR product with a one-year temporal resolution. The black line represents the linear fit of the AODs (T-test: $\alpha=0.013<0.05$).

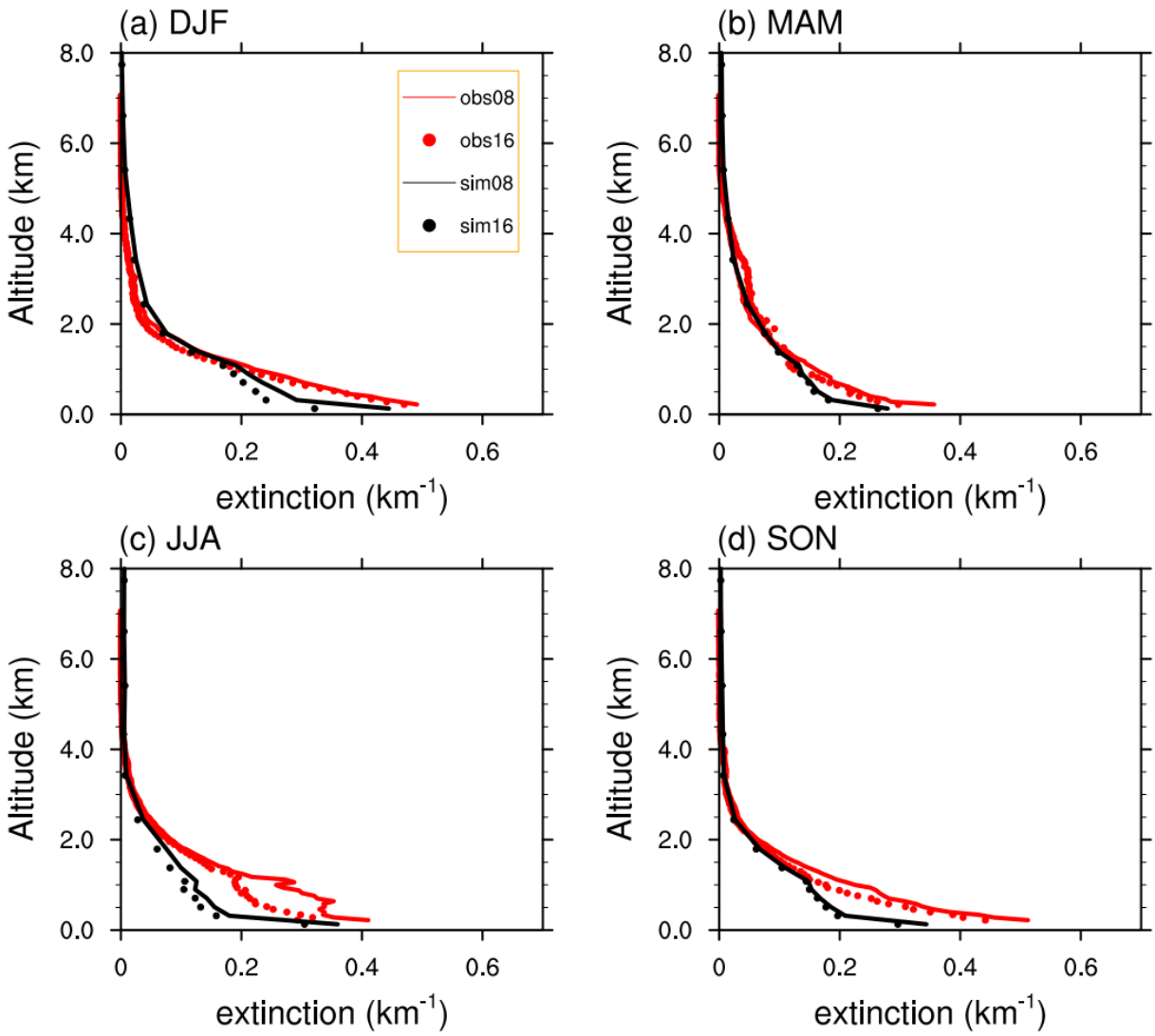

Fig. S7. Comparison of modeled vertical profiles of aerosol extinctions (sim08 and sim16) over eastern China in the Exp08 and Exp16 cases with the corresponding CALPSO measurements (obs08 and obs16). As the dust extinctions were found to be largely underestimated in our model compared to the dust subtype of CALIPSO observations (Fig. S8), their contribution was subtracted from the simulated and observed profiles.

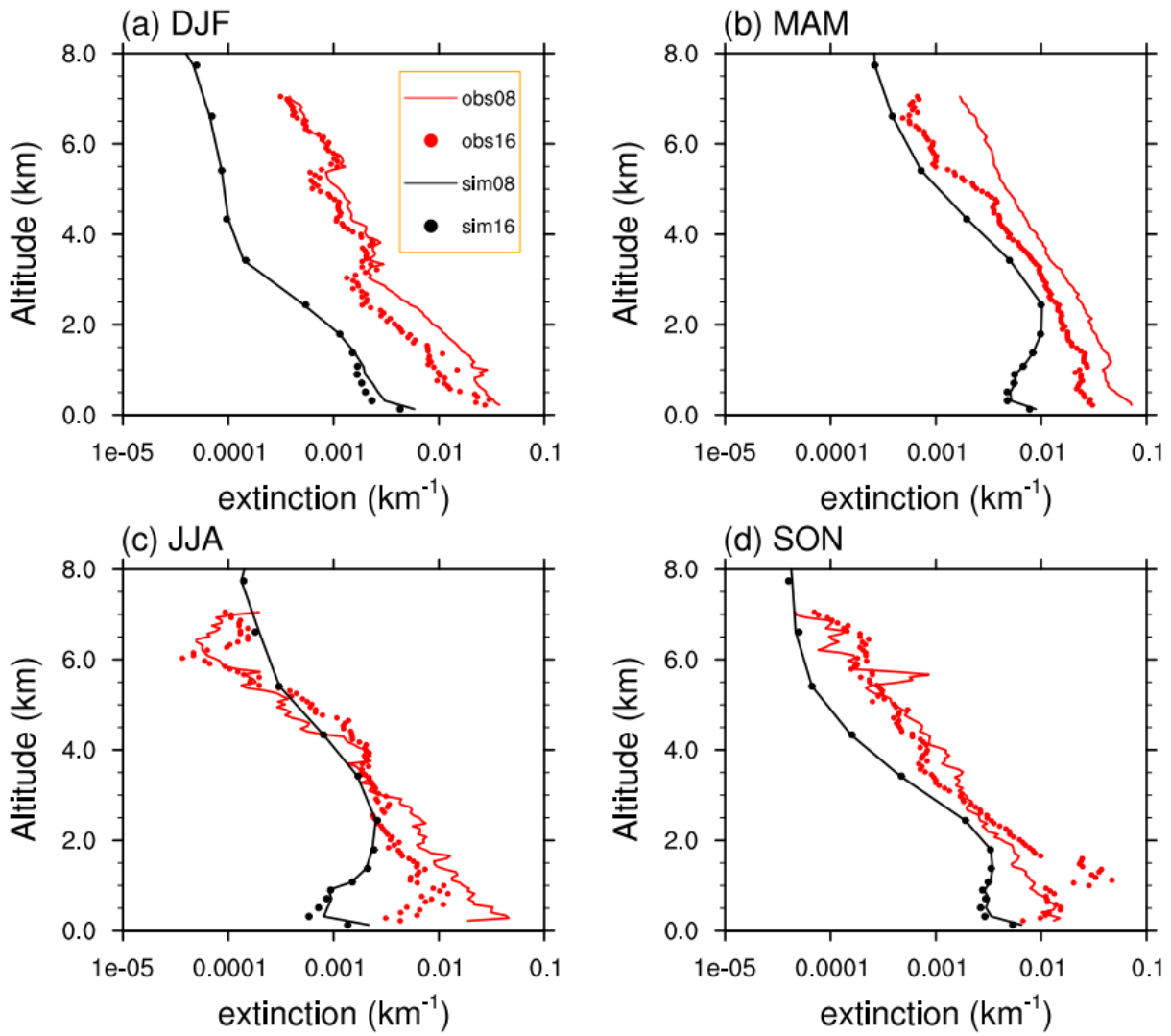

Fig. S8. Comparison of simulated seasonal mean dust extinction profiles (sim08 and sim16) with the corresponding CALIPSO data (obs08 and obs16) between 2008 and 2016. Note that the dust extinction observations shown here were derived from the "dust" subtype in the CALIPSO retrievals, while some natural and anthropogenic dust aerosols mixed with other components (like sea salts and biomass burning compounds) were classified as "polluted dust" and not included. Therefore, these dust extinction observations were a lower bound of total dust extinction and the gaps between simulations and observations should be even larger than those shown in the plots.

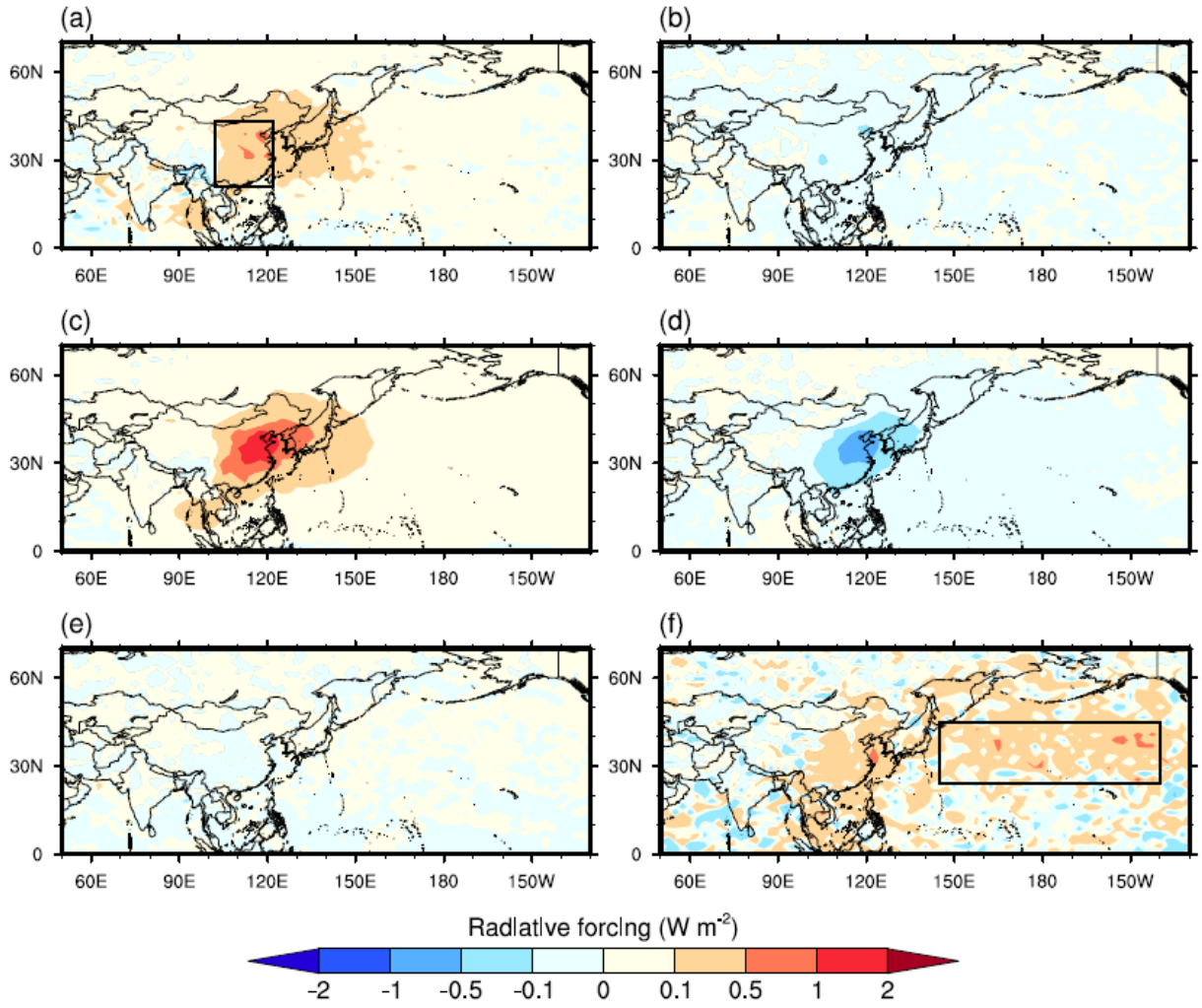

Fig. S9 Map of DRF from total aerosols (a), BC (b), sulfate (c), nitrate + ammonium (d), and OA + dust (e), and aerosol-induced clouds effects (f) due to the reduction of SO_2 emissions in China. DRF, direct radiative forcing.

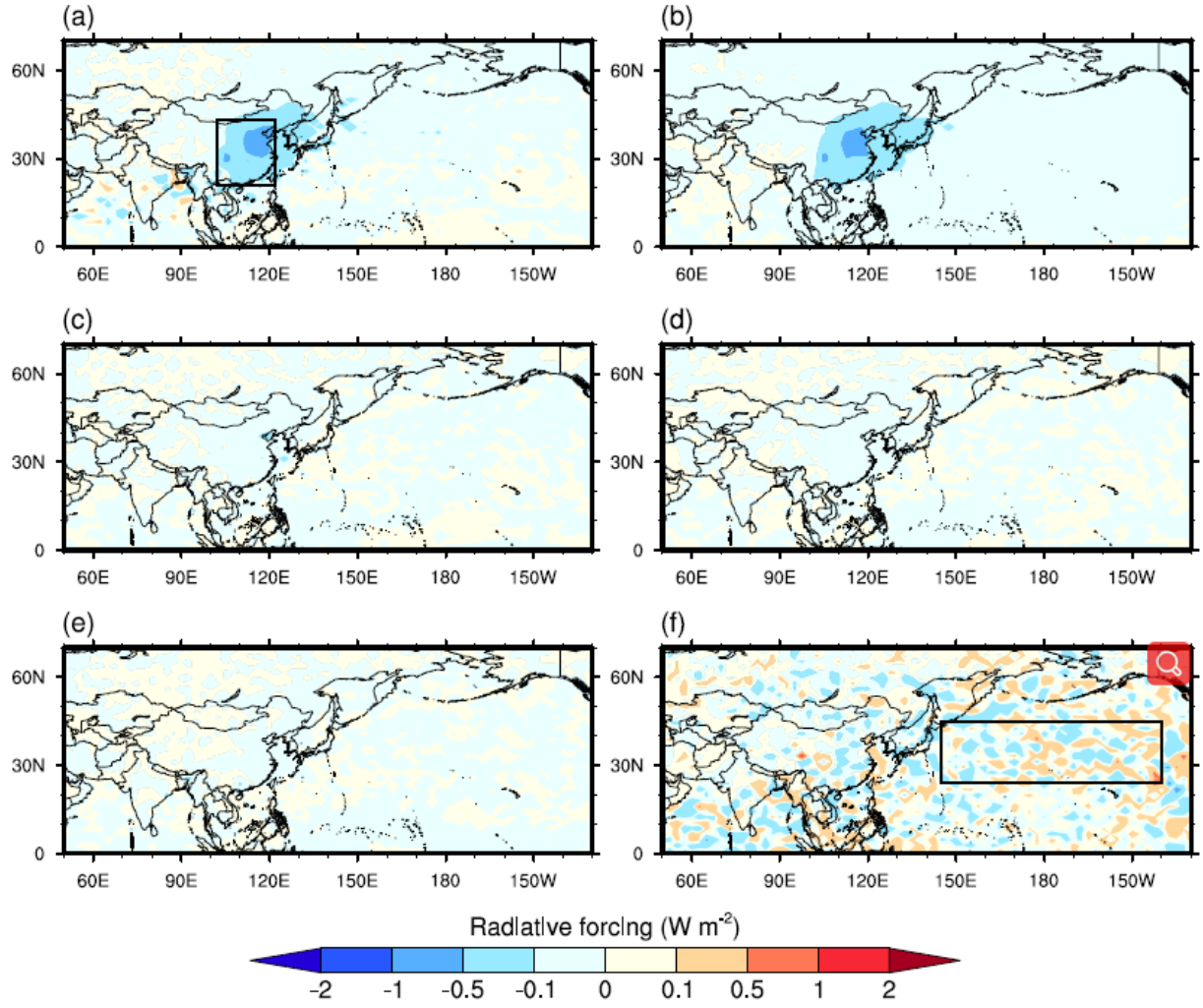

Fig. S10 The same with Fig. S9, but due to the reduction of BC emissions.

References

Ge, X., He, Y., Sun, Y., Xu, J., Wang, J., Shen, Y., and Chen, M.: Characteristics and Formation Mechanisms of Fine Particulate Nitrate in Typical Urban Areas in China, Atmosphere, 8, 10.3390/atmos8030062, 2017.

Geng, N., Wang, J., Xu, Y., Zhang, W., Chen, C., and Zhang, R.: PM2.5 in an industrial district of Zhengzhou, China: Chemical composition and source apportionment, Particuology, 11, 99-109, https://doi.org/10.1016/j.partic.2012.08.004, 2013.

Gu, J. X., Wu, L. P., Huo, G. Y., Bai, Z. P., Du, S. Y., Liu, A. X., and Xie, Y. Y.: Pollution Character and Source of Water-Soluble Inorganic Ions in PM2.5 over Tianjin (in Chinese), Environmental Monitoring in China, 29, 30-34, 2013.

Hu, W., Hu, M., Hu, W., Jimenez, J. L., Yuan, B., Chen, W., Wang, M., Wu, Y., Chen, C., Wang, Z., Peng, J., Zeng, L., and Shao, M.: Chemical composition, sources, and aging process of submicron aerosols in Beijing: Contrast between summer and winter, J. Geophys. Res.-Atmos, 121, 1955-1977, 10.1002/2015JD024020, 2016.

Huang, X. F., He, L. Y., Hu, M., Canagaratna, M. R., Sun, Y., Zhang, Q., Zhu, T., Xue, L., Zeng, L. W., Liu, X. G., Zhang, Y. H., Jayne, J. T., Ng, N. L., and Worsnop, D. R.: Highly time-resolved chemical characterization of atmospheric submicron particles during 2008 Beijing Olympic Games using an Aerodyne High-Resolution Aerosol Mass Spectrometer, Atmos. Chem. Phys., 10, 8933-8945, 10.5194/acp-10-8933-2010, 2010.

Kanaya, Y., Yamaji, K., Miyakawa, T., Taketani, F., Zhu, C., Choi, Y., Komazaki, Y., Ikeda, K., Kondo, Y., and Klimont, Z.: Rapid reduction of black carbon emissions from China: evidence from 2009-2019 observations on Fukue Island, Japan, Atmos. Chem. Phys. Discuss., 2019, 1-28, 10.5194/acp-2019-1054, 2019.

Li, K., Chen, L., White, S. J., Zheng, X., Lv, B., Lin, C., Bao, Z., Wu, X., Gao, X., Ying, F., Shen, J., Azzi, M., and Cen, K.: Chemical characteristics and sources of PM1 during the 2016 summer in Hangzhou, Environ. Pollut., 232, 42-54, https://doi.org/10.1016/j.envpol.2017.09.016, 2018.

Liu, M., Huang, X., Song, Y., Xu, T., Wang, S., Wu, Z., Hu, M., Zhang, L., Zhang, Q., Pan, Y., Liu, X., and Zhu, T.: Rapid SO2 emission reductions significantly increase tropospheric ammonia concentrations over the North China Plain, Atmos. Chem. Phys., 18, 17933-17943, 10.5194/acp-18-17933-2018, 2018.

Sun, J., Zhang, Q., Canagaratna, M. R., Zhang, Y., Ng, N. L., Sun, Y., Jayne, J. T., Zhang, X., Zhang, X., and Worsnop, D. R.: Highly time- and size-resolved characterization of submicron aerosol particles in Beijing using an Aerodyne Aerosol Mass Spectrometer, Atmos. Environ., 44, 131-140, https://doi.org/10.1016/j.atmosenv.2009.03.020, 2010.

Tong, D., Cheng, J., Liu, Y., Yu, S., Yan, L., Hong, C., Qin, Y., Zhao, H., Zheng, Y., Geng, G., Li, M., Liu, F., Zhang, Y., Zheng, B., Clarke, L., and Zhang, Q.: Dynamic projection of anthropogenic emissions in China: methodology and 2015-2050 emission pathways under a range of socio-economic, climate policy, and pollution control scenarios, Atmos. Chem. Phys., 20, 5729-5757, 10.5194/acp-20-5729-2020, 2020.

Wang, J., Ge, X., Chen, Y., Shen, Y., Zhang, Q., Sun, Y., Xu, J., Ge, S., Yu, H., and Chen, M.: Highly time-resolved urban aerosol characteristics during springtime in Yangtze River Delta, China: insights from soot particle aerosol mass spectrometry, Atmos. Chem. Phys., 16, 9109-9127, 10.5194/acp-16-9109-2016, 2016.

Wei, C., Wang, M. H., Fu, Q. Y., Dai, C., Huang, R., and Bao, Q.: Temporal Characteristics and Potential Sources of Black Carbon in Megacity Shanghai, China, J. Geophys. Res.-Atmos, 125, 10.1029/2019jd031827, 2020.

Xia, Y., Wu, Y., Huang, R.-J., Xia, X., Tang, J., Wang, M., Li, J., Wang, C., Zhou, C., and Zhang, R.: Variation in black carbon concentration and aerosol optical properties in Beijing: Role of emission control and meteorological transport variability, Chemosphere, 254, 10.1016/j.chemosphere.2020.126849, 2020.

Zhang, X. Y., Wang, Y. Q., Niu, T., Zhang, X. C., Gong, S. L., Zhang, Y. M., and Sun, J. Y.: Atmospheric aerosol compositions in China: spatial/temporal variability, chemical signature, regional haze distribution and comparisons with global aerosols, Atmos. Chem. Phys., 12, 779-799, 10.5194/acp-12-779-2012, 2012.

Zhang, Y., Sun, J., Zhang, X., Shen, X., Wang, T., and Qin, M.: Seasonal characterization of components and size distributions for submicron aerosols in Beijing, Science China Earth Sciences, 56, 890-900, 10.1007/s11430-012-4515-z, 2013.

Zhang, Y., Tang, L., Croteau, P. L., Favez, O., Sun, Y., Canagaratna, M. R., Wang, Z., Couvidat, F., Albinet, A., Zhang, H., Sciare, J., Prévôt, A. S. H., Jayne, J. T., and Worsnop, D. R.: Field characterization of the PM2.5 Aerosol Chemical Speciation Monitor: insights into the composition, sources, and

processes of fine particles in eastern China, Atmos. Chem. Phys., 17, 14501-14517, 10.5194/acp-17-14501-2017, 2017.